Sea Surface Backscatter Distortions of Scanning Radar Altimeter Ocean Wave Measurements

Edward J. Walsh and C. Wayne Wright
NASA Goddard Space Flight Center
Wallops Flight Facility
Wallops Island, VA 23337 USA

***Abstract*-This paper examines the distortions in the measured wave topography caused by sea surface backscatter variation within the 25 to 50 m antenna footprint of the 1° antenna beam of the NASA Scanning Radar Altimeter at its typical 1.5 to 3 km operating altitude and possible corrections to the directional wave spectra computed from the wave topography.**

I. INTRODUCTION

This paper deals with the effects of the finite beamwidth of a beam-limited scanning radar altimeter on its ability to measure the properties of ocean waves. Figure 1 shows the basic measurement geometry of the NASA Scanning Radar Altimeter (SRA). It swept a radar beam of 1° (two-way) half-power width across the aircraft ground track within ±22° of the perpendicular to the aircraft wings to produce a swath equal to 0.8 of the aircraft height, simultaneously measuring the backscattered power at its 36 GHz (8.3 mm) operating frequency and the range to the sea surface at 64 positions, separated by 0.7° in incidence angle.

In realtime, the slant ranges are multiplied by the cosine of the off-nadir incidence angles (including the effect of aircraft roll attitude) to determine the vertical distances from the aircraft to the sea surface. These distances are subtracted from the aircraft height to produce a sea-surface elevation map, which is displayed on a monitor in the aircraft to enable real-time assessments of data quality and wave properties. The SRA generally operated at 1.5 to 3 km altitude and produced the raster lines of sea surface topography at about 16 Hz.

This paper examines the distortions of the measured wave topography caused by the 1° antenna beam and the possibility of correcting the directional wave spectra computed from the wave topography. The directional wave spectra are represented in terms of ocean wave propagation vectors in wave number space, so the spectral variance densities are referenced to the directions in which the waves are traveling.

II. WAVE MEASUREMENT GEOMETRY

Figure 2 shows the wave measurement geometry of the SRA for waves propagating perpendicular to the aircraft track for two boresight incidence angles. To make this analysis as general as possible, the transmitted pulse is idealized to be Gaussian in shape and 6 ns in half-power width for an effective range extent of 0.9 m. Similarly, the two-way antenna beam is assumed to be Gaussian in cross section with a half-power width of 1°.

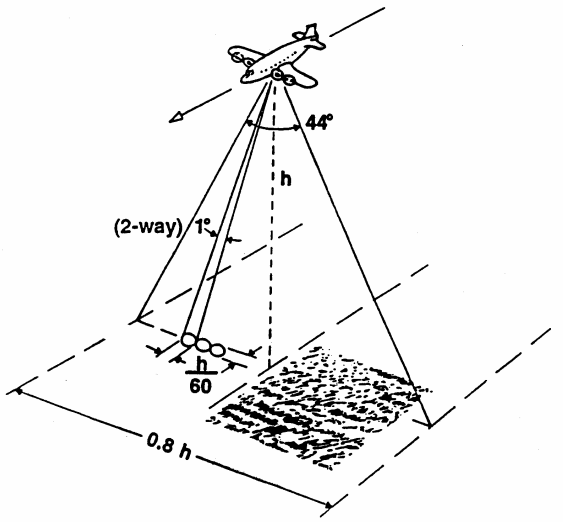

Figure 1. SRA basic measurement geometry.

The top panel of Figure 2 shows, in proper proportion for the SRA at 1.5 km height, circles (nearly straight, horizontal lines) representing the leading and trailing half-power points of the 6 ns transmitted pulse approaching the sea surface when the antenna is boresighted at nadir. The antenna boresight is indicated by the solid line perpendicular to the pulse and the energy density varies laterally along the pulse as a function of the antenna gain. The antenna half-power points (±0.5°) are indicated by the dashed lines and the antenna 0.1 power points (±0.91°) are indicated by the dotted lines.

The sea surface wave topography depicted in Figure 2 is an infinitely long-crested sinusoid of 50 m length and 2 m crest-to-trough height, propagating perpendicular to the aircraft track. Even though the sea surface elevation at the antenna boresight is 1 m above sea level, the centroid of the power received by the SRA for that geometry will indicate a lower surface elevation. When the back of the pulse (half-power width) is still illuminating the crest of the 50-m wave, the front of the pulse will extend almost to mean sea level. The centroid range of the backscattered power would be longer than the range to the crest and the crest height would appear lower. If a wave trough were at the boresight, the opposite would be true and the overall wave height would appear smaller. This spatial filtering effect by the antenna footprint which will reduce the apparent amplitude of waves at nadir. The effect would be minimal for waves of 250 m or longer and severe for wavelengths shorter than the antenna footprint.

1-4244-0115-1/06/$20.00 ©2006 IEEE

Report Documentation Page

Form Approved
OMB No. 0704-0188

1. REPORT DATE	2. REPORT TYPE	3. DATES COVERED
01 SEP 2006	**N/A**	**-**

4. TITLE AND SUBTITLE	5a. CONTRACT NUMBER
Sea Surface Backscatter Distortions of Scanning Radar Altimeter Ocean Wave Measurements	5b. GRANT NUMBER
	5c. PROGRAM ELEMENT NUMBER
6. AUTHOR(S)	5d. PROJECT NUMBER
	5e. TASK NUMBER
	5f. WORK UNIT NUMBER
7. PERFORMING ORGANIZATION NAME(S) AND ADDRESS(ES) **NASA Goddard Space Flight Center Wallops Flight Facility Wallops Island, VA 23337 USA**	8. PERFORMING ORGANIZATION REPORT NUMBER
9. SPONSORING/MONITORING AGENCY NAME(S) AND ADDRESS(ES)	10. SPONSOR/MONITOR'S ACRONYM(S)
	11. SPONSOR/MONITOR'S REPORT NUMBER(S)

12. DISTRIBUTION/AVAILABILITY STATEMENT
Approved for public release, distribution unlimited

13. SUPPLEMENTARY NOTES
See also ADM002006. Proceedings of the MTS/IEEE OCEANS 2006 Boston Conference and Exhibition Held in Boston, Massachusetts on September 15-21, 2006, The original document contains color images.

14. ABSTRACT

15. SUBJECT TERMS

16. SECURITY CLASSIFICATION OF:			17. LIMITATION OF ABSTRACT	18. NUMBER OF PAGES	19a. NAME OF RESPONSIBLE PERSON
a. REPORT	b. ABSTRACT	c. THIS PAGE			
unclassified	**unclassified**	**unclassified**	**UU**	**4**	

Standard Form 298 (Rev. 8-98)
Prescribed by ANSI Std Z39-18

The bottom panel of Figure 2 shows the same SRA pulse and wave profile, but near the edge of the measurement swath for an antenna boresight at 20° off-nadir. The transmitted pulse is shown just interacting the sea surface at the left edge of the figure (-40 m). The near side of the wave whose crest is at the boresight has a lower incidence angle than at the crest, and lower still than for the far side of the crest. The variation of backscattered power with incidence angle will weight the shorter ranges on the near side of the crest more heavily than the longer ranges on the far side of the crest and the centroid range will be shorter than the range to the wave crest located at the boresight of the antenna. There is no alternative but to assign this shorter range to the antenna boresight angle, which will result in a higher than actual wave crest determination.

The reverse would happen if a wave trough were at the antenna boresight in the bottom panel of Figure 2. The far side of the trough would have a lower incidence angle and more backscattered power than the near side of the trough. The centroid range would be longer than the range to the trough at the antenna boresight. But ascribing that longer range to the boresight angle would indicate a deeper trough than was actually the case.

The general effect of the finite antenna beamwidth (compared to the negligible width of a scanning airborne laser beam) is to reduce the apparent height of ocean waves propagating across the aircraft track when they are observed at nadir and to increase their apparent height when they are viewed off-nadir. The magnitude of the off-nadir distortion increases with decreases in either the ocean wavelength or the sea surface mean square slope (mss), which increases the variation of backscattered power with incidence angle.

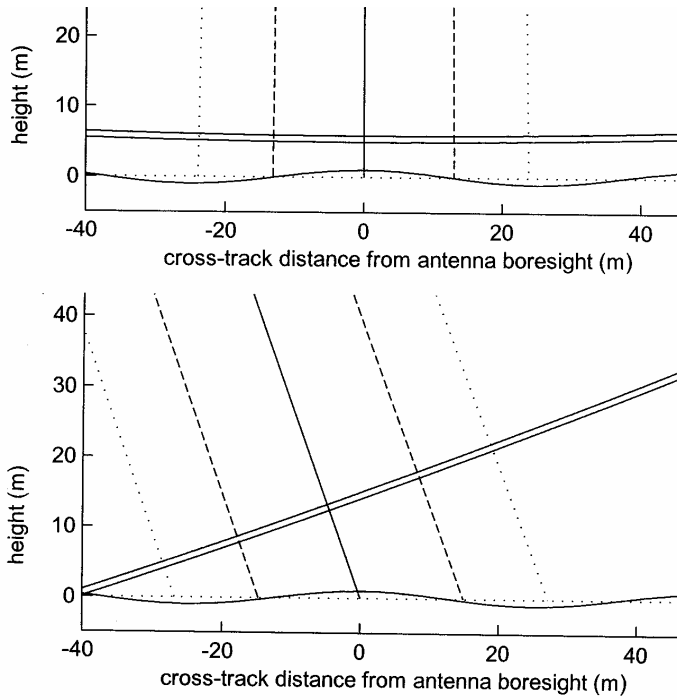

Figure 2. Nadir and 20° off-nadir SRA pulse and antenna geometry with respect to a long-crested wave of 50 m length and 2 m crest to trough height.

The reduction in the apparent amplitude of waves measured at nadir is independent of the wave propagation direction. But waves propagating parallel to the aircraft track are minimally affected by the tilt-modulation enhancement effect when observed off-nadir because the cross-track incidence angle variation would be along the wave crest and change only by the 1° beamwidth and not be compounded by ocean wave curvature.

Although it is impossible to apply corrections to individual wave measurements because the slope of the portion of the wave within the antenna footprint is not resolved, statistical corrections can applied to the directional wave spectra computed from the topography.

III. Hurricane Wave Measurements

For eight hurricane seasons (1998-2005) the SRA flew aboard one of the NOAA WP-3D hurricane research aircraft to provide the first and only wave field topographic maps and directional wave spectrum information throughout the inner core of hurricanes [1, 2, 3]. The multiple flight directions and altitudes employed during a flight into Hurricane Ivan on 9 September 2005 provided data to demonstrate the effect of wave geometry on the SRA measurements.

Figure 4 shows average directional wave spectra computed from approximately 27 km along-track segments (3000 scan lines) of SRA wave topography. The centers of the wave topography segments are indicated by the three circles on the southwest flight line in the vicinity of 15.6°N, 73.3°W. The SRA antenna scans perpendicular to the aircraft heading, indicated by the short, thick radial from the spectral origin.

Figure 5 shows average directional wave spectra computed from approximately 20 km along-track segments (3000 scan lines) of SRA wave topography from the southeast flight segment. The centers of those wave topography segments are indicated by the three circles in the vicinity of 15°N, 73.1°W. The same scan line span covered less distance of the southeast segment because the aircraft was flying crosswind instead of downwind as was the case on the southwest segment.

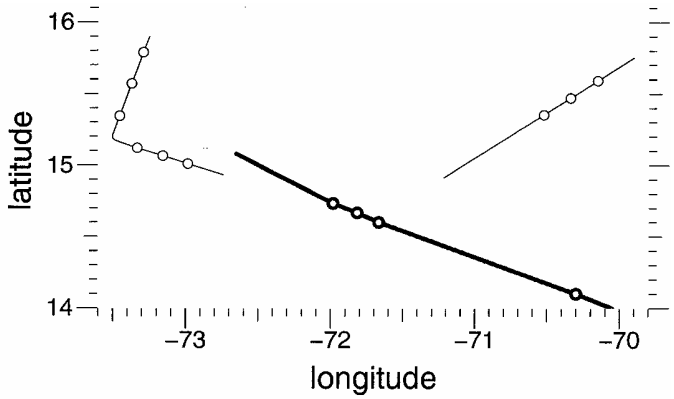

Figure 3. The thick line indicates the track of Hurricane Ivan. The three thick circles on the hurricane track line in the vicinity of 71.8W indicate the locations of the eye fixes made by the NOAA aircraft during the flight on 9 September 2004. The thin lines indicate flight segments of the NOAA aircraft and the thin circles indicate the centers of data spans used to generate the data shown in Figures 4 through 7.

The long radials extending from the origin in Figures 4 and 5 indicate the downwind vector at the aircraft altitude. The short radials indicate the aircraft heading, which was nearly perpendicular to the wave propagation direction in Figure 4 and nearly parallel to it in Figure 5.

Since the SRA antenna scan plane is perpendicular to the aircraft wings, the 250-m wavelength dominant waves were propagating across the swath on the southwest flight segment (Figure 4) and subjecting the SRA to the wave tilt-modulation effect depicted in Figure 2. But for the southest flight segment (Figure 5) the same dominant wave system was propagating along the aircraft track and no tilt-modulation effect would be expected.

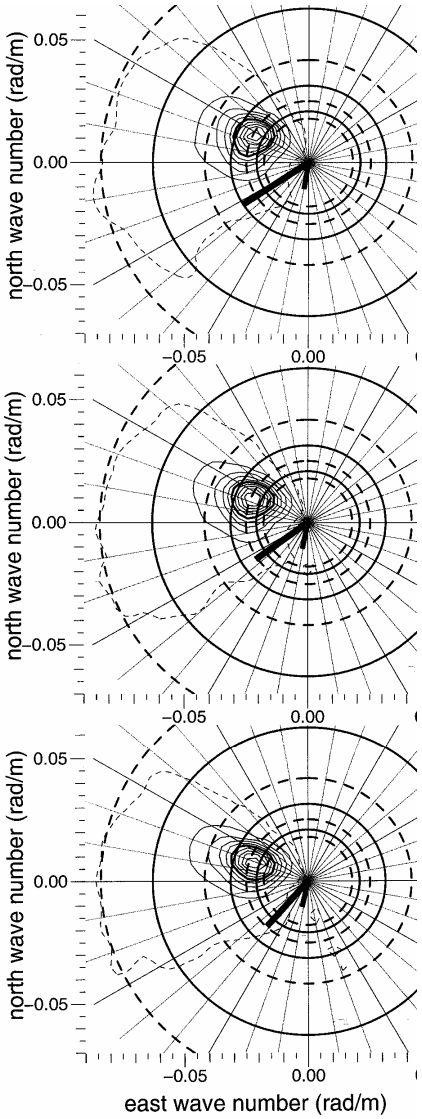

Figure 4. Nine solid contours linearly distributed from the 10% to the 90% levels in spectral variance density relative to the spectral peak. The dashed contour is at the 1% level. The solid circles correspond to ocean wavelengths of 100, 200 and 300 m (outer to inner). The four dashed circles correspond to wavelengths of 75, 150, 250, and 350 m. The long radial indicates the wind vector at the aircraft 1.5 km height (divided by 1000 before plotting) and the short radial indicates the aircraft heading. The dominant waves had approximately 250 m length and were propagating toward about 290°. The significant wave heights for the three spectra were 5.4 m, 5.2 m and 4.7 m (top to bottom, southwest flight segment starting from 15.8°N, 73.3°W).

Figure 6 shows wave spectra generated from groups of 3000 SRA scan lines along the southwest segment on the right side of Figure 3 in the vicinity of 15.5°N, 70.3°W. In this region there was a bimodal wave system whose centroid direction of propagation was approximately perpendicular to the aircraft heading so the waves were approximately propagating across the swath and the scattering geometry was similar to that shown in Figure 2.

Figure 7 shows the variation in the surface elevation standard deviation of each group of 3000 along-track elevation values measured by the SRA as a function of off-nadir incidence angle (cross-track position). The standard deviations were multiplied by four so the plotted values could be thought of as the SRA estimate of the sea surface significant wave height as a function of the off-nadir incidence angle of the antenna boresight.

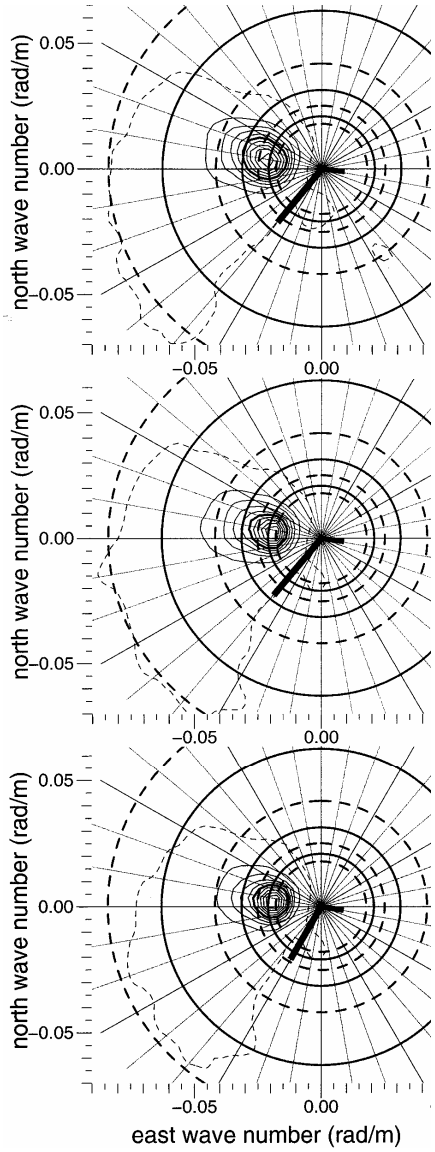

Figure 5. Same format as Figure 4. Aircraft height was also 1.5 km. The significant wave heights for the three spectra were 4.2 m, 4.5 m and 5.1 m (top to bottom, southeast flight segment starting from 15.1°N, 73.3°W).

Ideally, the SRA would produce the same elevation standard deviation for every antenna beam incidence angle since an actual wave profile over any 20 km along-track distance should encounter a sufficient number of waves that lateral variations in the wave field would be averaged out, but that is not the case. The top panel of Figure 7 shows that the measured standard deviation increased as the incidence angle increased, as suggested by the wave tilt-modulation discussion surrounding Figure 2.

The middle panel of Figure 7 corresponds to the spectra shown in Figure 5 where the SRA was scanning parallel to the wave crests and troughs, not perpendicular to them. In this instance the standard deviation shows almost no variation within ±15° as one would expect in the absence of the wave tilt-modulation effect.

The abrupt increase in standard deviation near the edges of the swath is due to the wind-driven waves suggested by the dashed contour in Figure 5, which were propagating across the SRA swath. Although lower in wave height, they were steep and short in wavelength and the tilt-modulation effect became very large as the incidence angle increased near the edge of the swath.

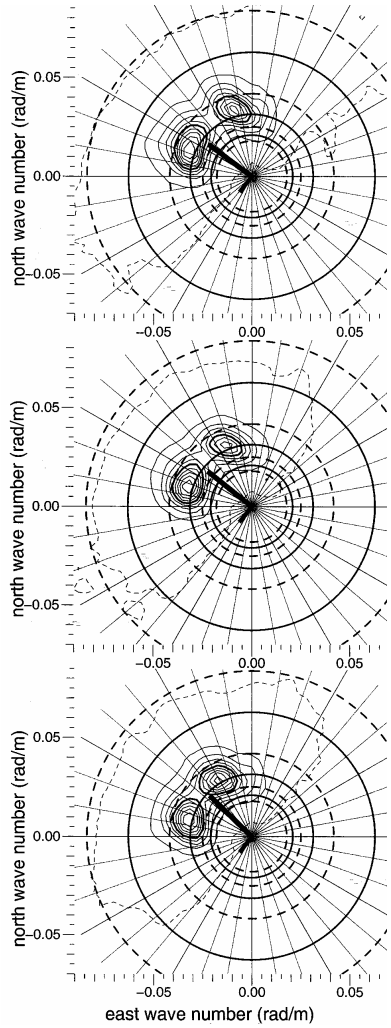

Figure 6. Same format as Figure 4. Aircraft height was 2.5 km and significant wave heights for the three spectra were 4.8 m, 5.4 m and 6.1 m (top to bottom, southwest flight segment starting from 15.6°N, 70.15°W).

The bottom panel of Figure 7 corresponds to the spectra of Figure 6 and represents a similar situation to that of Figure 4. The measured surface elevation standard deviation begins to increase immediately with incidence angle, similar to the top panel of Figure 7, but the increase is more pronounced because the aircraft was 1 km higher and the antenna footprint was larger. The wave tilt-modulation effect varies inversely as mss and the ratio of ocean wavelength to antenna footprint.

ACKNOWLEDGMENTS

The NASA Physical Oceanography Program and the Office of Naval Research CBLAST-Hurricane program supported this effort. The NOAA Hurricane Research Division and Aircraft Operations Center provided a great deal of assistance.

REFERENCES

[1] C. W. Wright, E. J. Walsh, D. Vandemark, W. B. Krabill, A. Garcia, S. H. Houston, M. D. Powell, P. G. Black, and F. D. Marks, "Hurricane directional wave spectrum spatial variation in the open ocean," *J. Phys. Oceanogr.,* vol. 31, 2001, pp. 2472-2488.

[2] E. J. Walsh, C. W. Wright, D. Vandemark, W. B. Krabill, A. W. Garcia, S. H. Houston, S. T. Murillo, M. D. Powell, P. G. Black, F. D. Marks, "Hurricane directional wave spectrum spatial variation at landfall," *J. Phys. Oceanogr.,* vol. 32, 2002, pp. 1667-1684.

[3] Il-Ju Moon, I. Ginis, T. Hara, H. L. Tolman, C. W. Wright and E. J. Walsh, "Numerical simulation of sea surface directional wave spectra under hurricane wind forcing," *J. Phys. Oceanogr.,* vol. 33, 2003, pp. 1680-1706.

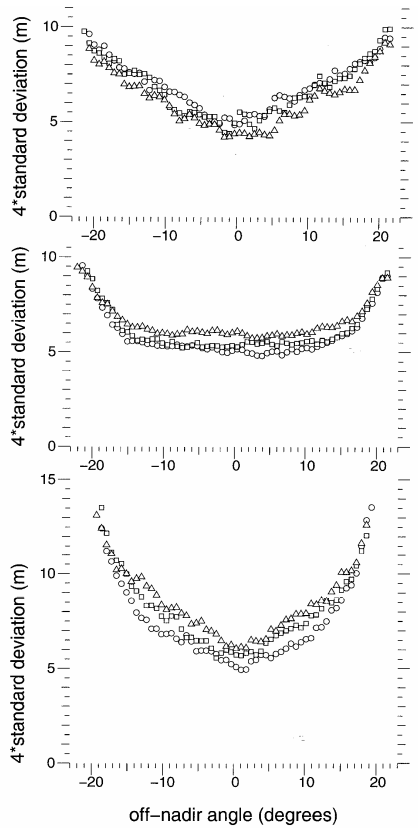

Figure 7. Surface elevation standard deviation measured by the SRA as a function of antenna off-nadir incidence angle for the SRA topography used to generate the spectra shown in Figures 4 (top panel), 5 (middle panel) and 6 (bottom panel). Within each panel the symbols correspond to the top (circle), middle (square), and bottom (triangle) spectra shown in Figures 4, 5, and 6.